Supplementary Information (SI)

Nanoscale wetting and energy transmission at solid-liquid interfaces

John A. Tomko,[†] David H. Olson,[‡] Ashutosh Giri,[‡] John T. Gaskins,[‡] Brian F. Donovan,[¶] Sean M. O'Malley,[§] and Patrick E. Hopkins[*,†]

[†]*Department of Materials Science and Engineering, University of Virginia, Charlottesville, VA 22904, USA*

[‡]*Department of Mechanical and Aerospace Engineering, University of Virginia, Charlottesville, VA 22904, USA*

[¶]*Department of Physics, United States Naval Academy, Annapolis MD 21402, USA*

[§]*Department of Physics, Rutgers University - Camden, Camden, NJ 08102, USA*

[||]*Department of Physics, University of Virginia, Charlottesville, VA 22904, USA*

E-mail: phopkins@virginia.edu

Manuscript title	Nanoscale wetting and energy transmission at solid-liquid interfaces
Authors	John A. Tomko, David H. Olson, Ashutosh Giri, John T. Gaskins, Brian F. Donovan, Sean M. O'Malley, and Patrick E. Hopkins
Page S3	Comparison of phonon transmission coefficients for thick (80 nm) and thin (20 nm) Au films
Page S4	Example fits to picosecond acoustic signals for various liquids
Page S6	1) Phonon transmission coefficient as a function of measured contact angle for various liquids and 2) shadowgraphy images to display contact angle measurements

1 Sample Preparation

The metal films are electron beam evaporated on amorphous SiO_2 substrates; the substrates are cleaned prior to deposition with ethanol and methanol, followed by O_2 plasma, and then N_2 blasted. We follow a similar procedure prior to the pump-probe measurements with varying liquids, where the Au films are rinsed, plasma cleaned, and again blasted with N_2. Additionally, we determine the film thickness with profilometry measurements; the values obtained from profilometry are in agreement with the values obtained via the picosecond acoustic oscillations. These thicknesses are measured both before and after submersion in the respective liquids to assure the film has not delaminated in the probed area.

2 Picosecond Acoustic Measurements

As noted in the primary manuscript, we measure the picosecond acoustic oscillations for Au films that have 75 nm and 20 nm thicknesses. In the case of our 75 nm Au films, we use a reflection geometry for our pump-probe experimental setup. In this case, the beam propagates through the 1 mm SiO_2 substrate and interacts with the 75 nm film at normal incidence; it is then reflected

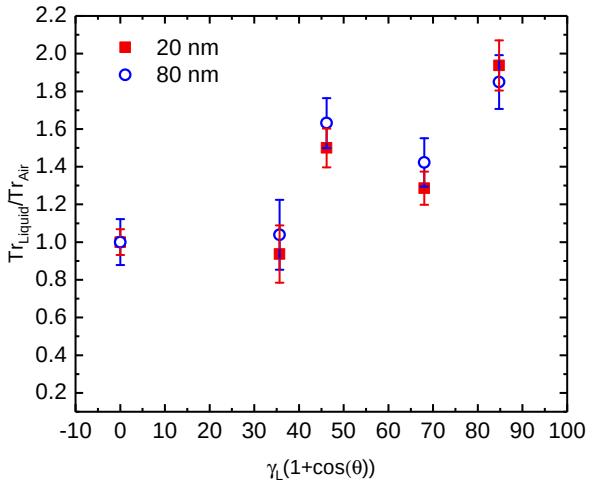

Figure S1: Comparison of the transmission coefficient, normalized to that of air, for varying Au/liquid interfaces. We find that the 20 nm (red open circles) and 80 nm (blue squares) are in good agreement, implying the two optical pump-probe techniques, reflection and transmission, provide similar transmission coefficients that are unaltered by optical nonlinearities or other acoustic signals in the sample.

back into a balanced photodiode with the alterations to discussed in the primary manuscript. The beam does not interact with the liquid layer on the opposing side of the metal film as it is entirely reflected or absorbed at this thickness of gold.

In the case of measuring our 20 nm Au films, these alterations are not necessary. Rather, as these films are partially transparent at the probe wavelength of 800 nm, we simply move the photodiode behind the probed sample and rely on the same sample geometry (i.e., amorphous SiO_2/20 nm Au/liquid).

As shown in Fig. S1, the two methods show good agreement when considering the normalized transmission coefficient and scale linearly with other measures of interfacial energy transport (i.e., the measured ablation threshold[1]). This implies both methods provide versatile measurement techniques of acoustic transmission coefficients between varying media. In a transmission geometry, the beam does not undergo nonlinear phenomena, including in the case of FC70, a common nonlinear media. We attribute this to the low peak powers associated with our pulses at 80 MHz. Further, in a reflection geometry, where we measure the decay of the signal in resonance with the brillouin

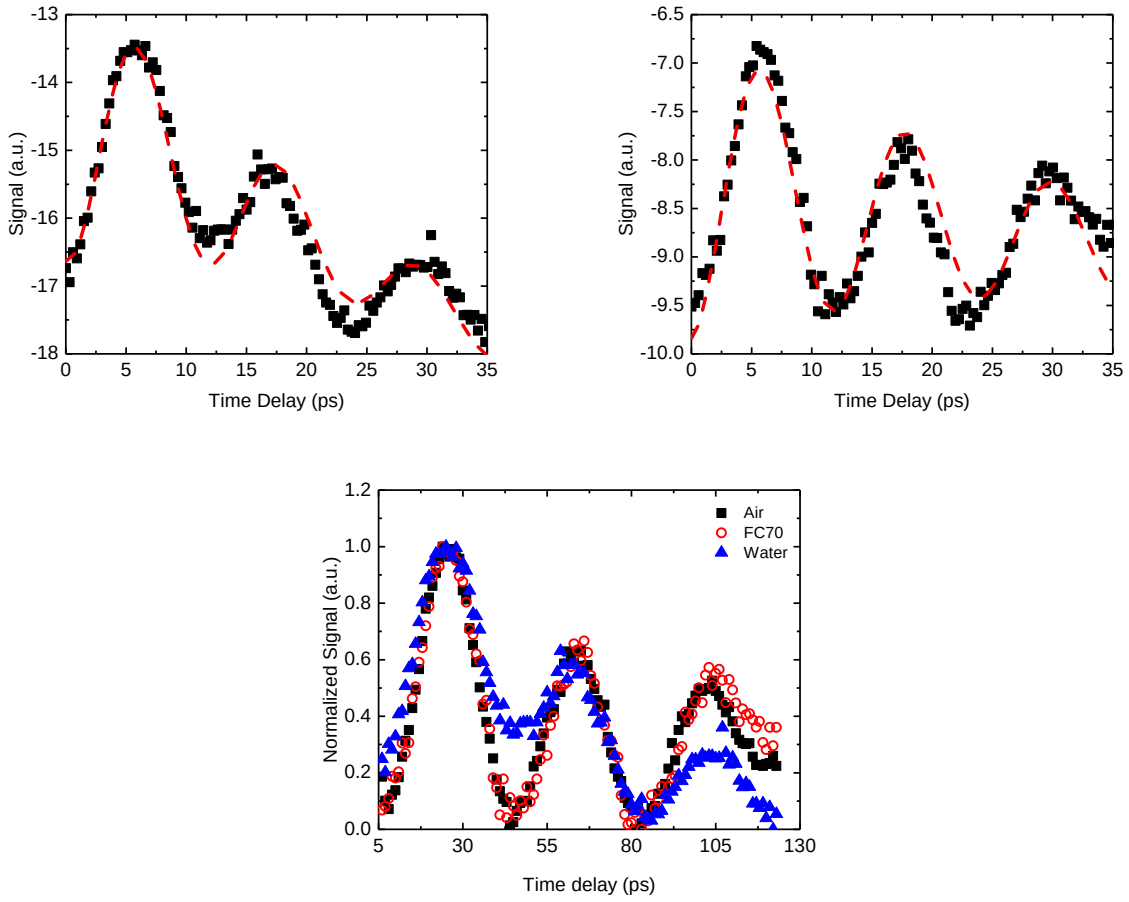

Figure S2: Example fits for Eq. (1) in the manuscript to Au/water (top) and Au/FC70 (middle) interfaces for 20 nm thin films. The bottom figure shows the normalized signal for air, FC70, and water interfaces, where there is negligible difference seen in the decay for either air or FC70.

scattering in the underlying transparent substrate, we find that this decay remains indicative of the transmission coefficient.

Examples of the decay, and fitted curve from Eq. (1) of the manuscript, are shown in Fig. S2. As can be seen, there is minimal difference between the decay of the picosecond acoustic oscillations for 20 nm Au films submerged in FC70 and films in ambient conditions. Conversely, there is a clear dampening effect when the films are submerged in water.

3 Wetting Measurements

We measure the contact angle for the varying liquids on Au films through shadowgraphy imaging. In all cases, a 5 μL drop is placed on the Au film; we find that acoustic phonon transmission does not scale solely with the contact angle, as shown in the primary manuscript. To consider true solid-liquid adhesion, we consider the Young Dupré equation, where the liquid surface energy, γ_L, is accounted for in addition to the measured contact angle. We obtain these values, for the respective liquids, from literature.[2–5] Note, in cases such as ethanol, γ_L is for pure EtOH, whereas the experimentally measured EtOH contains approximately 5% water based on turbidity tests;[6] this is accounted for in the error associated with the work of adhesion calculations. The shadowgraphy images are shown in S4.

4 Ablation Threshold Measurements

The ablation threshold measurements and specifics of the laser system used are discussed in previous works.[1,7] Here, we measure the single-shot ablation threshold of Au films using a 25 ps, Nd:YAG laser at its fundamental wavelength of 1064 nm. The Au films for these measurements have a thickness of 200 nm and are supported by amorphous SiO_2 substrates. We choose this thickness to ensure the dominant resistance in the system is that of the Au/liquid interface rather than that of the Au/substrate interface. Regardless, our previous study has found the Au/liquid interface, even in thin systems, to be an accessible thermal pathway for these pulse durations.

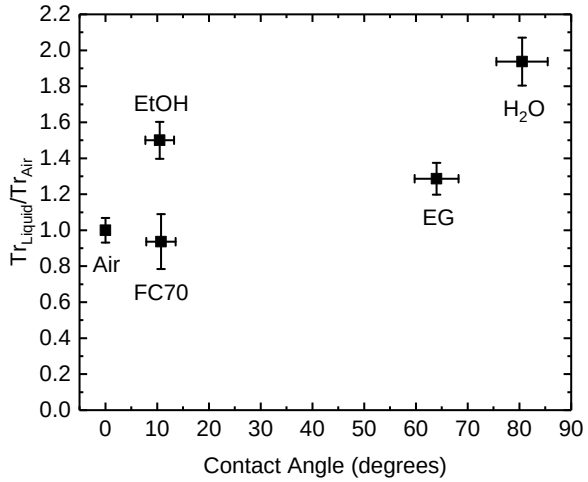

Figure S3: Measured transmission coefficient of acoustic modes for 20 nm Au films in various media, normalized by the coefficient associated with an Au/air interface, as a function of measured contact angle.

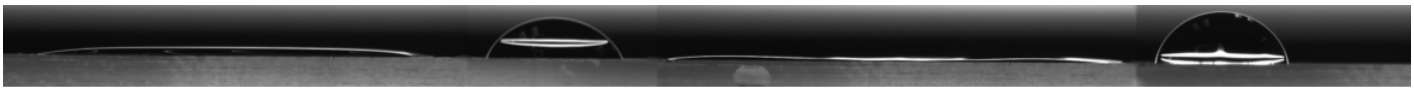

Figure S4: Shadowgraphy images for the various media on Au films. Left to right: FC70, ethylene glycol, ethanol, and water. Note, the measured acoustic transmission for each of these Au/liquid interfaces scales left to right, indicating a clear lack of trend with contact angle.

We note the discrepency between our previous measurement of ablation thresholds of thin Au films[1] and nominal values provided within this work. To simplify the measurement, we define the threshold as the fluence required to completely remove the thickness of the film. In this work, to minimize the role of film-substrate interfacial effects, we use 200 nm Au films for the ablation experiments to approximate 'bulk' properties; this is roughly three times greater than our previous study. Hence, the energy necessary for complete removal would be predicted to be approximately three times greater, as well. From this perspective, the values are in good agreement for Au films on SiO_2 in ambient conditions. Of course, when measuring the ablation threshold of bulk targets, surface restructuring of any thickness is accounted for, and thus approaches the thin film limit as found prior.[7]

References

(1) Tomko, J. A.; Giri, A.; Donovan, B. F.; Bubb, D. M.; O'Malley, S. M.; Hopkins, P. E. Energy confinement and thermal boundary conductance effects on short-pulsed thermal ablation thresholds in thin films. *Physical Review B* **2017**, *96*, 014108.

(2) Vargaftik, N. B.; Volkov, B. N.; Voljak, L. D. International Tables of the Surface Tension of Water International Tables of the Surface Tension of Water. *Journal of Physical and Chemical Reference Data* **1983**, *12*, 817.

(3) Vazquez, G.; Alvarez, E.; Navaza, J. M. Surface Tension of Alcohol + Water from 20 to 50 C. *Journal of Chemical and Engineering Data* **1995**, *40*, 611–614.

(4) Tsierkezos, N. G.; Molinou, I. E. Thermodynamic Properties of Water + Ethylene Glycol at 283.15, 293.15, 303.15, and 313.15 K. *Journal of Chemical and Engineering Data* **1998**, *43*, 989–993.

(5) Wong, T.-s.; Kang, S. H.; Tang, S. K. Y.; Smythe, E. J.; Hatton, B. D.; Grinthal, A.; Aizen-

berg, J. Bioinspired self-repairing slippery surfaces with pressure-stable omniphobicity. *Nature* **2011**, *477*, 443–447.

(6) Hall, J. A simple, rapid method for measuring the percentage of water in alcohols used for dehydrating tissues. *Biotechnic & Histochemistry* **2001**, *76*, 41–42.

(7) Tomko, J.; Naddeo, J. J.; Jimenez, R.; Tan, Y.; Steiner, M.; Fitz-Gerald, J. M.; Bubb, D. M.; O'Malley, S. M. Size and polydispersity trends found in gold nanoparticles synthesized by laser ablation in liquids. *Physical Chemistry Chemical Physics* **2015**, *17*, 16327–16333.